REVIEW ARTICLE | FOCUS
PUBLISHED ONLINE: 30 NOVEMBER 2010 | DOI: 10.1038/NPHOTON.2010.239
nature photonics

X-ray free-electron lasers

Brian W. J. McNeil[1]* and Neil R. Thompson[2]

With intensities 10^8–10^{10} times greater than other laboratory sources, X-ray free-electron lasers are currently opening up new frontiers across many areas of science. In this Review we describe how these unconventional lasers work, discuss the range of new sources being developed worldwide, and consider how such X-ray sources may develop over the coming years.

In classical electromagnetism, a charged particle radiates energy in the form of electromagnetic radiation when it accelerates. This effect is the principle behind many useful sources of radiation across a wide range of the electromagnetic spectrum. The free-electron laser (FEL) is one such source, which, due to a Doppler frequency up-shifting of emitted radiation by relativistic electrons, is particularly well-suited to generating short-wavelength X-rays. There are currently no alternative sources that have such high pulse energies and short durations. This Review gives a brief historical perspective on X-ray FELs, describes the operating principle of this technology, summarizes the current status of shorter-wavelength FEL facilities and explores the potential for future development.

Electromagnetic energy may be extracted from the kinetic energy of a relativistic electron beam by propagating it along the axis of a periodic lattice of alternating magnetic dipolar fields, known as an 'undulator'. This forces the beam to undulate transversely, thus causing the electrons to emit electromagnetic radiation. The fundamental wavelength emitted is proportional to λ_u/γ^2, where λ_u is the undulation period, typically a few centimetres, and γ is the relativistic Lorentz factor of the electrons, which is typically several thousand for X-ray emission. The first theoretical works describing such undulator radiation were reported by Ginzburg[1] and Motz[2] in the late 1940s to early 1950s. Experiments at Stanford in 1953 generated the first incoherent undulator radiation at visible and millimetre wavelengths, with an estimated peak power of the latter reaching ~10 W, as reported by Motz, Thon and Whitehurst[3]. A few years later, Phillips conducted research on an undulator microwave source called the 'ubitron'[4]. In the ubitron, $\gamma \gtrsim 1$ and there is minimal Doppler up-shifting of the radiation wavelength from that of the undulator period. However, Phillips noted that two of the main qualitative features common with a FEL interaction were present in his experiments: a density modulation (bunching) of the electron beam along its (axial) direction of propagation, and radiation energy extraction from the axial kinetic energy of the beam. It was not until 1971 that Madey[5], who was unaware of the earlier microwave work of Phillips, published a seminal theory of the FEL that described a small gain process in a relativistic electron beam/undulator system, which he hypothesized could generate coherent X-ray radiation. It was probably this potential that sparked significant interest in the FEL throughout the research community. The first amplification[6] and lasing[7] from a FEL was demonstrated in a small-gain infrared FEL oscillator system at Stanford a few years later. Around this time, it was shown by Colson[8] and Hopf *et al.*[9] that Madey's original quantum description of the FEL interaction could be described classically. From the late 1970s a body of work was developed that described classically what is now termed the high-gain regime of FEL operation[10–17]. In fact, this regime has many theoretical similarities with earlier works on the generation of microwaves[18]. In this high-gain regime, the radiation power increases exponentially as the electron beam and radiation co-propagate along the FEL undulator, and an initially small source, which may originate as noise, can be amplified by many orders of magnitude before the process saturates. In the X-ray there is therefore no need for potentially troublesome mirrors to form an oscillator cavity. The FEL functions as a single-pass amplifier, generating peak powers of the order of 10^{10} W in pulses lasting tens of femtoseconds. Most of the present X-ray FEL facilities and designs are based on this type of interaction, which has been made possible by many advances in electron beam generation and acceleration over the past few decades. More extensive texts are available in addition to the original research cited in this Review, including works by Murphy and Pellegrini[19], Bonifacio *et al.*[20] and Saldin, Schneidmiller and Yurkov[21], among others.

In essence, the high-gain FEL interaction is a positive feedback process — the electrons emit radiation, which affects their position (phase) and thus causes them to emit with greater coherence. The effect is a collective (also called cooperative) process, and is a form of collective Thompson scattering. X-ray FELs operate in the Compton regime, in which space–charge effects are negligible. Several other free-electron generators of electromagnetic radiation have a very similar underlying mechanism that, in certain limits, may be described formally by the same set of equations presented below[22]. More generally, the high-gain FEL interaction has strong similarities with other collective particle–radiation interactions: the collective atomic recoil laser[23,24]; collective Rayleigh scattering from linear dielectric particles[25]; and collective scattering from the electron–hole plasma in semiconductors[26]. The high-gain FEL interaction can also be classified as a type of Kuramoto-like 'collective synchronization'[27].

Spontaneous undulator radiation

Before describing the collective, self-consistent FEL interaction, we first consider radiation emission in the absence of any FEL interaction — spontaneous undulator radiation.

The trajectory of an electron and the full radiation field it emits in an undulator are obtained from classical electromagnetism[28]. An intuitive approach allows calculation of the important on-axis radiation wavelengths generated by considering a simple time-of-flight argument. A co-propagating radiation wavefront will always move ahead of an electron. By considering simple wave interference, only those wavelengths that propagate ahead of the electron by an integer number of wavelengths in one undulator period, as shown in Fig. 1, will constructively interfere after many such periods. These wavelengths, $\lambda_n = \lambda_1/n$ (where $n = 1, 2, 3...$), are defined as being 'resonant', with other wavelength components tending to interfere destructively. The time taken for an electron propagating along the undulator axis with mean speed $\bar{v}_z$ to travel one undulator period, $t' = \lambda_u/\bar{v}_z$, is the same time a resonant wavefront takes to

[1]Scottish Universities Physics Alliance, Department of Physics, University of Strathclyde, Glasgow G4 0NG, UK. [2]ASTeC/Cockcroft, Daresbury Laboratory, Warrington WA4 4AD, UK. *e-mail: b.w.j.mcneil@strath.ac.uk

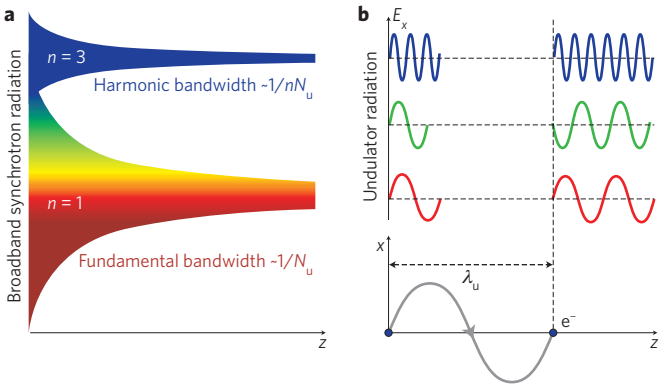

Figure 1 | An undulator selects only certain resonant wavelengths of the radiation emitted by an electron. a, The lower plot shows an electron trajectory over one undulator period, λ_u. The upper plot shows the electric fields E_x for two resonant wavelengths λ_n at the fundamental ($n = 1$; red) and third harmonics ($n = 3$; blue). A non-resonant electric field is also shown (green). The fundamental and third harmonics are phase-matched with the electron after one undulator period — these constructively interfere over many periods. The non-resonant field is not phase-matched and will destructively interfere over many periods. **b**, Plot showing how the radiation spectrum evolves from a broadband synchrotron source to the distinct resonant wavelengths of undulator radiation as a function of the undulator length $z = N_u\lambda_u$ over many periods.

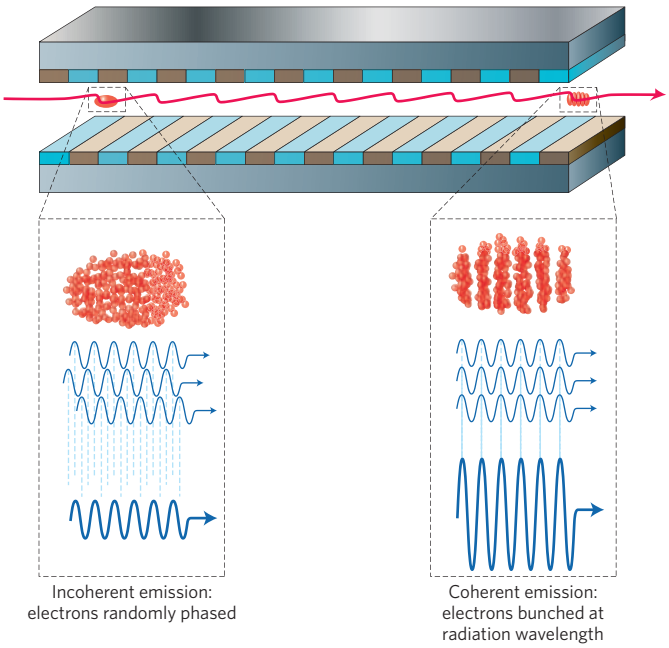

Figure 2 | FEL operating principle. When electrons enter the undulator, their initially random phases ensure that mostly incoherent radiation is emitted at the resonant radiation wavelength (left). Because the electrons interact collectively with the radiation they emit, small coherent fluctuations in the radiation field grow and simultaneously begin to bunch the electrons at the resonant wavelength. This collective process continues until the electrons are strongly bunched towards the end of the undulator (right), where the process saturates and the electrons begin to de-bunch.

travel the distance $\lambda_u + n\lambda_n$; that is, $t' = (\lambda_u + n\lambda_n)/c$, where c is the speed of light in vacuum. By equating these expressions, the following relation for the resonant wavelengths is obtained[28]:

$$\lambda_n = \frac{\lambda_u}{n}\left(\frac{1-\bar{v}_z/c}{\bar{v}_z/c}\right) \approx \frac{\lambda_u}{2n\gamma^2}(1+\bar{a}_u^2) \quad \text{for } n = 1, 2, 3...$$

where $\bar{v}_z \approx c(1 - (1 + \bar{a}_u^2)/2\gamma^2)$ and $\bar{a}_u$ is the root-mean-squared undulator parameter proportional to the undulator period and magnetic field, which is typically $1 \lesssim \bar{a}_u \lesssim 5$. For a given fundamental wavelength λ_1, this expression can be inverted to obtain the resonant z-component of the mean electron velocity, giving $\bar{v}_z = ck_1/(k_1 + k_u)$.

A more detailed analysis[28] shows that only the fundamental and odd harmonic wavelengths of the radiation ($n = 1, 3, 5...$) are in fact emitted on-axis, and for an helical undulator, in which the electron motion forms a spiral along the z axis, only the fundamental harmonic has strong emission on-axis. The wavelength can be tuned by changing either the electron energy (by varying γ) or the undulator parameter $\bar{a}_u$.

The power emitted by the electrons in an undulator is given by:

$$P \propto \left|\sum_{j=1}^{N} E_j e^{i\varphi_j}\right|^2 = \sum_{j=1}^{N} E_j^2 + \left|\sum_{\substack{j=1 \\ j\neq k}}^{N}\sum_{k=1}^{N} E_j E_k e^{i(\varphi_j+\varphi_k)}\right|^2$$

where φ_j are the relative phases of the emitted radiation electric fields E_j, with the number of electrons $N \gg 1$. For a system with uncorrelated phases, the second sum of $\sim N^2$ terms tends to destructively interfere. This is what happens in normal incoherent 'spontaneous' sources of undulator radiation, and the total power emitted is approximately equal to the sum of the powers from the N independent scattering electrons. To tap into the potentially much larger coherent N^2 term, the phases of the electric fields must be correlated; that is, $\varphi_j \approx \varphi_k$ for all electrons. Put simply, the electron sources must be periodically bunched at the resonant radiation wavelength. This is what the FEL interaction does, as shown schematically in Fig. 2. We shall now demonstrate how the high-gain FEL interaction does this by describing how the electrons interact collectively in the combined undulator/radiation fields.

The high-gain FEL interaction

To describe the high-gain FEL interaction, coupled equations that follow the electron motion and radiation generation self-consistently are required. The Lorentz equation describes the forces on each electron resulting from the combined undulator and radiation fields, and Maxwell's wave equation describes the electric field of the radiation as driven by the transverse electron current induced by the fields.

First, it is useful to consider how the transversely oscillating electrons bunch at the resonant wavelength in a fixed plane wave field of constant amplitude. An electron's rate of change of energy may be written as:

$$\frac{d(\gamma mc^2)}{dt} = -e\mathbf{E}\cdot\mathbf{v} \propto E\bar{a}_u\left[\sin((k_1+k_u)z - w_1 t) + \sin((k_1-k_u)z - w_1 t)\right]$$

Although the second term has a phase velocity of $v_{ph} > c$, the first term has a phase velocity of $v_{ph} = ck_1/(k_1 + k_u) < c$. This is exactly the mean resonant electron velocity obtained previously for the resonant undulator radiation; that is, $\bar{v}_z = v_{ph}$, which shows that, neglecting the fast oscillatory second term with $v_{ph} > c$, an electron

NATURE PHOTONICS DOI: 10.1038/NPHOTON.2010.239

interacting with a resonant radiation field can have a slow exchange of energy with the field over many undulator periods. Electrons that are separated by half a radiation period have opposite rates of energy change — half of the electrons lose energy while the other half gains energy. This process causes the electrons to bunch at the radiation wavelength, allowing a coherent interaction between the electrons and the radiation. The forces that bunch the electrons can be considered as a series of periodic potential wells (Φ) travelling at the resonant electron velocity, which is referred to as a 'ponderomotive' potential. However, in a constant field, the bunching process cannot describe any energy gain of the radiation field. The gain process can be described by lifting this restriction of a constant radiation field and considering how the electron bunching and field growth self-consistently drive each other in an exponentially unstable feedback loop.

The steady-state model

The self-consistently coupled equations that describe a FEL are shown in Box 1. They are written here in their universally scaled form[17], in the one-dimensional, plane-wave limit, for a potential well approximately one-radiation-wavelength long. The first two differential equations are derived from the Lorentz force equation for the electrons and, for a radiation phase of $\phi = -\pi/2$, are formally identical to the equations of simple pendula of angle θ from stable equilibrium[8]. The other two equations are derived from Maxwell's wave equation for the radiation electric field, and describe the evolution of the field envelope of amplitude a and phase ϕ as driven by the transverse current of the electrons. ρ is a fundamental scaling parameter known as the FEL or Pierce parameter[17,18], and gives a measure of the strength and scaling of the electron–radiation FEL coupling and its saturated efficiency. Clearly, several simplifying assumptions have been made in deriving these equations[17].

The initial electron phases θ_{j0} are uniformly distributed over the range $(0, 2\pi]$. Thus, $\langle\cos(\theta_0 + \phi_0)\rangle = \langle\sin(\theta_0 + \phi_0)\rangle = 0$, and the field is not driven. If, in addition, the initial field amplitude a_0 is zero then there are no bunching forces on the electrons and the system is stable. Now consider what happens if the system has a small initial field $a_0 \ll 1$, with phase $\phi_0 = 0$, as shown in Fig. 3.

The electrons experience a small force that tends to slightly bunch them symmetrically about the bottom of the potential. The field amplitude is not driven because, for electron bunching about $\theta = 3\pi/2$, the source term $\langle\cos(\theta + \phi_0)\rangle = 0$. However, the field phase ϕ is driven and increases because its source $-1/a_0\langle\sin(\theta + \phi_0)\rangle > 0$. Even though the electron bunching about $\theta = 3\pi/2$ will initially be small — that is, $\langle\sin(\theta + \phi_0)\rangle \ll 1$ — the initial field amplitude a_0 is itself very small, so that the rate of change of ϕ is significant. It is this driving of the radiation phase to larger values that lies at the heart of the instability. Although the electrons bunch about $\theta = 3\pi/2$, the increasing radiation phase means that $\langle\theta\rangle + \phi \gtrsim 3\pi/2$ and the radiation field amplitude begins to increase because its source term $\langle\cos(\theta + \phi)\rangle > 0$. The increasing field amplitude raises the bunching forces on the electrons closing the positive feedback loop, and so the exponential instability takes off. Once the field amplitude has grown to $a \approx 1$, the electrons achieve maximum bunching, the driving of the phase slows down and the system enters the nonlinear saturated regime.

As the electrons become strongly bunched at the fundamental harmonic, there is also a strong nonlinear driving of harmonic bunching components[20] $b_n = \langle\exp(-in\theta)\rangle$, which prove very useful in extending the radiation generation to shorter wavelengths (see, for example, refs 29–33).

Linearization of these equations[17] reveals an exponential instability in both the scaled field amplitude a and the fundamental electron bunching parameter b_1. The radiation power is given by $P(z) \approx P_0/9\ \exp(\sqrt{3}z/l_g)$, until the interaction saturates. Here the initial power P_0 can be approximated from analysis by Kim[34], and the gain length l_g defines the exponential growth rate. The scaled radiation power is given by $a^2 \approx P/\rho P_e$, where P_e is the electron beam power, so that at saturation, when the scaled power is $a^2 \approx 1$, ρ is seen to be a measure of the efficiency of the interaction, with typical values in the X-ray regime of $10^{-4} \lesssim \rho \lesssim 10^{-3}$. The scaling also shows that the energy spread of the electron beam at saturation is $\sigma_\gamma \approx \rho$, and the saturated power scales as $\sqrt[3]{I^4}$, which demonstrates the collective nature of the interaction. It also becomes clear through this

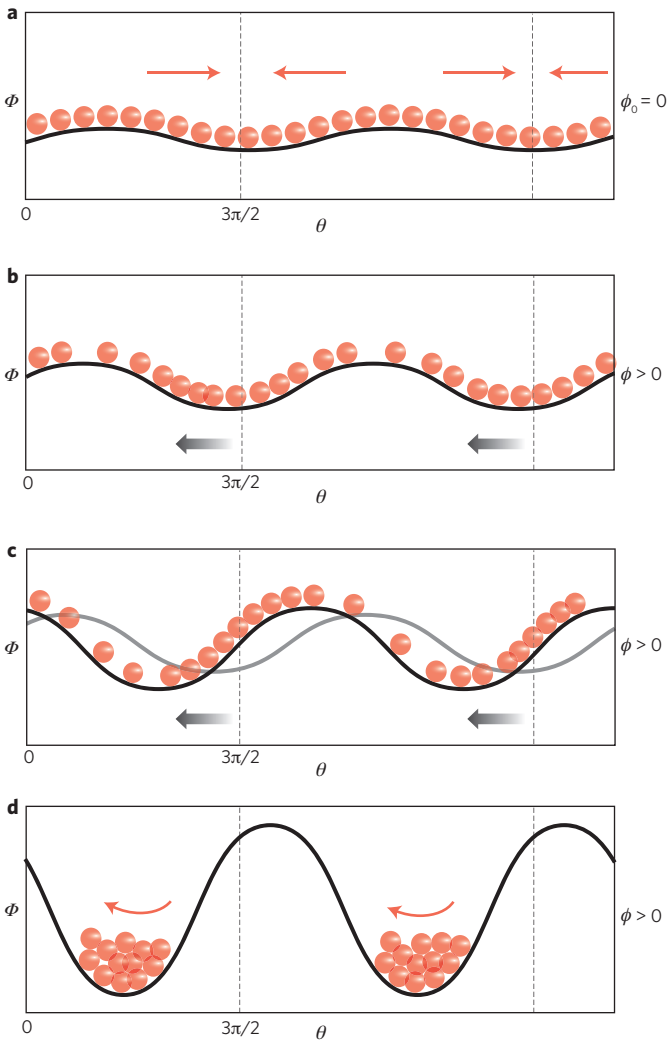

Figure 3 | The high-gain FEL mechanism in the rest frame of the electron beam, which is propagating left to right. a–d, A small radiation field of initial phase $\phi_0 = 0$ is applied to the electrons at the start of the undulator (**a**). Φ represents two ponderomotive potential wells. The forces on the electrons (red arrows) tend to induce a small electron bunching about the phases $\theta = 3\pi/2$ and $\theta = 7\pi/2$. This small bunching drives the radiation phase ϕ, thus shifting the ponderomotive wells Φ of phase $(\theta + \phi)$ to the left (**b**). The weakly bunched electrons are now raised in potential energy and begin to 'fall' into the potential well, thus losing kinetic energy to the radiation field and increasing the depth of the potential well. This radiation phase shifting, electron bunching and energy exchange from electrons to the field continues exponentially in a type of 'inverse surfing' of the electrons (**c**) until the phase growth in ϕ slows down when the field becomes large. The system saturates when the now strongly bunched electrons begin to re-gain kinetic energy from the potential and re-absorb energy from the field — the electrons begin to 'surf' (**d**).

Table 1 | Current X-ray facilities that are either operational (O), under construction (C) or undergoing advanced technical design work (D). 'Accelerator technology' refers to either normal conducting (NC) or superconducting (SC) accelerating cavities. The wavelength given is the minimum proposed. Emittance values (ε_n) are estimates for C- and D-type facilities.

Name	Location	Status	Type	Energy (GeV)	ε_n (μm)	λ_{min} (nm)	Maximum pulses per second	Radiation polarization control
LCLS[51]	USA	O	NC	14	1	0.12	120	No
FLASH[101]	Germany	O	SC	1.2	<2	4.45	8×10^3	No
XFEL[52]	Germany	C	SC	17.5	1.4	0.10	27×10^3	Yes
XFEL/SPring-8[53]	Japan	C	NC	8	0.8	0.10	60	No
FERMI@Elettra[57]	Italy	C	NC	1.7	1	4	50	Yes
SwissFEL[56]	Switzerland	D	NC	6	0.4	0.1	100	Yes
PAL XFEL[102]	Korea	D	NC	10	1	0.1	60	No
LCLS-II[103]	USA	D	NC	14	1	0.6	120	Yes
SPARX[104]	Italy	D	NC	2.4	1	0.6	100	Yes
FLASH-II[54]	Germany	D	SC	1.2	1–1.5	4	10	No

analysis that the quality of the electron beam is of critical importance. If there is an initial electron energy spread approaching the maximum, which occurs at a FEL saturation of $\sigma_\gamma \gtrsim \rho$, then the FEL interaction is greatly reduced.

Higher-order effects

The steady-state analysis, which assumes an electron beam of infinite duration and uniform density, is generally not valid in a real X-ray FEL. The electron pulses typically injected into the undulator have up to ~1 nC of charge and durations of tens of femtoseconds, which correspond to several tens of thousands of radiation wavelengths at 1 Å. The radiation field propagates (or 'slips') through the electron pulse at one fundamental wavelength λ_1 per undulator period. When the system starts from noise, different regions of the radiation–electron interaction can evolve with no phase correlation, and the longitudinal coherence of the output is greatly reduced from the Fourier transform limit. This behaviour is analogous to amplified spontaneous emission in conventional lasers[35], and in FELs has been referred to as self-amplified spontaneous emission (SASE), with basic properties described by Bonifacio *et al.*[36]. Regions of the radiation pulse that develop phase correlation — and therefore temporal coherence — are determined by the relative slippage length between the electrons and radiation over one gain length. This is known as the cooperation length[37], $l_c = \lambda_1/4\pi\rho$. Autonomous regions of width $\sim 2\pi l_c$ evolve in SASE, within which a temporally coherent radiation pulse or 'spike' develops. For an electron pulse of length l_b there will be approximately $l_b/2\pi l_c$ of these phase-uncorrelated spikes — over 100 in a typical X-ray FEL design.

Several design criteria must be met for successful FEL operation, with most relating to the quality of the electron pulse as it enters the undulator. Here we will not discuss the huge technical advances and innovations in pulse compression, transport and acceleration that have occurred over the past few decades to enable the generation of sufficiently high-quality electron pulses. Each FEL accelerator system is unique in many respects, and a flavour of the requirements for the Linac Coherent Light Source (LCLS) may be found in a presentation by Emma[38]. Instead, here we focus on the parameters at the FEL undulator entrance and how they affect the FEL interaction.

Of critical importance is the normalized transverse beam emittance[39] $\varepsilon_n = \gamma\varepsilon$, where ε is the transverse emittance and is a measure of the transverse phase space occupied by the beam. An example of a beam with zero emittance would be one in which all electrons propagate parallel to each other. ε_n is related to the expression for the normalized beam brightness $B_n = I/\pi^2\varepsilon_n^2$, which is analogous to the radiance (often termed brightness) of a light source.

A limit on the normalized beam emittance for ensuring good spatial (transverse) coherence from sources of spontaneous undulator radiation was derived by Kim[40], giving $\varepsilon_n < \gamma\lambda_1/4\pi$. Although this expression was derived for systems without gain, it turns out that it is also a requirement for the successful operation of a high-gain amplifier FEL.

For beams with non-zero emittance, focusing is required to offset any beam divergence. Focusing can be achieved using a variety of different methods[41,42], and causes the electrons to undergo transverse betatron oscillations[43] in a 'focusing channel' through the undulator. The oscillations are characterized by the beta-function $\beta = \lambda_\beta/2\pi$, where λ_β is the betatron oscillation period, which is usually significantly larger than the undulator period. A constant-strength focusing channel gives a 'matched beam' of constant radius[43] $\sigma_e = \sqrt{\varepsilon_n\beta/\gamma}$. From this scaling and the scaling rules given for ρ and l_g in Box 1, a larger ε_n decreases the coupling parameter ρ and so increases the interaction gain length l_g. Furthermore, during their betatron oscillations, electrons oscillate in and out of resonance with the resonant radiation wavelength. This effect can be described by an effective electron beam energy spread that increases with ε_n and so further disrupts the electron bunching and FEL gain processes[44].

Radiation diffraction from the electron beam will tend to reduce the electron–radiation coupling. In a working FEL amplifier this is partially compensated for by two FEL gain processes[45]. The rate of change of the radiation phase is greater at the centre of the electron beam (where there is greater coupling), and thus the radiation wavefronts distorts to focus the radiation in a type of 'optical guiding' similar to that of an optical fibre. In addition, the amplification of the radiation more than compensates for losses due to diffraction, in what has been referred to as 'gain guiding'.

The spatial coherence limit $\varepsilon_n < \gamma\lambda_1/4\pi$ also emerges from a less rigorous consideration that balances the competing requirements on the beam radius: an increase in beam radius reduces diffraction effects, whereas a decrease causes a rise in the coupling parameter ρ and so a reduction in the effective energy spread due to betatron oscillations. A balance is sufficiently achieved when $\varepsilon_n \lesssim \gamma\lambda_1/4\pi$. This relation gives a rough rule-of-thumb estimate of the electron energy/wavelength possibilities and shows, for example, that the

Box 1 | The universally scaled FEL equations

From the Lorentz force equation:

$$\frac{d\theta_j}{d\bar{z}} = p_j; \quad \frac{dp_j}{d\bar{z}} = -2a\cos(\theta_j + \phi)$$

From Maxwell's wave equation:

$$\frac{da}{d\bar{z}} = \langle\cos(\theta + \phi)\rangle; \quad \frac{d\phi}{d\bar{z}} = -\frac{1}{a}\langle\sin(\theta + \phi)\rangle$$

These equations describe the coupled electron and radiation fields for one ponderomotive potential in a FEL. They are universally scaled[17] in that there are no free parameters, with the scaling giving physical insight as discussed in the main text. The parameters of the scaling are given as follows:

$j = 1...N$ is the number of electrons;

$\bar{z} \equiv z/l_g$ is the scaled distance through the undulator;

$l_g = \lambda_u/4\pi\rho$ is the nominal interaction gain length;

$\theta_j \equiv (k_1 + k_u)z - \omega_1 t_j$ is the phase of an electron in the ponderomotive potential;

$p_j \equiv (\gamma_j - \gamma_r)/\rho\gamma_r$ is the scaled electron energy of the jth electron;

γ_r is the resonant beam energy for fundamental radiation wavelength λ_1;

a is the scaled radiation field envelope;

ϕ is the radiation field phase;

$$\langle ... \rangle \equiv 1/N \sum_{j=1}^{N} (...)_j$$

is an average over all electrons in the potential;

$$\rho = \frac{1}{2\gamma}\left(\frac{I}{I_A}\left(\frac{\lambda_u \bar{a}_u f_B}{2\pi\sigma_e}\right)^2\right)^{1/3}$$

is the Pierce or FEL parameter;

$I_A \approx 17$ kA is the Alfvén current;

I is the electron beam current;

σ_e is the electron beam cross-sectional radius;

$f_B = J_0(\xi) - J_1(\xi)$, where $J_n(x)$ are Bessel functions; and

$\xi = \bar{a}_u^2/2(1 + \bar{a}_u^2)$.

minimum wavelength achievable decreases with normalized emittance, for a given beam energy. Clearly, the smaller the normalized emittance, the better. Note that the localized emittance (referred to as the 'slice' emittance) can vary significantly along the beam to give hot-spots where lasing can occur.

Two further criteria must be met for lasing. First, the electron beam must propagate straight through the undulator. For example, a transverse drift of 10–20% can significantly disrupt the FEL interaction, and this requires a deviation of <5 μm over the entire ~130 m length of undulators in the LCLS. Second, fluctuations in the undulator parameter $\bar{a}_u$ must be small enough such that period-to-period dephasing of the electrons with respect to the radiation does not occur. To meet these criteria at X-ray wavelengths requires significant diagnostic alignment procedures together with good thermal and mechanical stability[46,47].

Many of the above effects are discussed in more detail by Huang and Kim[48]. A body of work, summarized by Xie and described in ref. 48, led to an analytic 3D description that modifies the interaction gain length l_g to include these effects, which is very useful for FEL design optimization.

Recent research is detailed in the works of Geloni *et al.*, Saldin *et al.*, and Vartanyants and Singer in the compendium of ref. 49, which includes a statistical description of FEL emission and more detail of the coherence properties.

Current source developments

Current X-ray FEL projects[50] range from paper outlines to fully operational facilities. Table 1 lists those that are either operational or at an advanced stage of development.

It is interesting to compare the technology used by each of the three hard-X-ray FELs currently operational or under construction — LCLS[51], XFEL[52] and XFEL/SPring-8[53] — and examine how these affect the facility capability and size. The LCLS uses a ~1 km section of a relatively old linear accelerator at the SLAC National Accelerator Laboratory in California, USA. Utilizing this well-understood system allowed rapid progress towards the first operation of a hard-X-ray FEL. Because the linear accelerator operates at room temperature with copper radiofrequency accelerating cavities, the pulse repetition rate is limited to a maximum of 120 Hz. Current operation is at 30 Hz, with 120 Hz operation anticipated in the near future[51].

In contrast, the European XFEL and FLASH-II[54] at DESY in Hamburg, Germany, will use the same type of superconducting accelerating cavities as FLASH, which has served as the test-bed for many of the technologies employed at the European XFEL. Such cavities allow for repetition rates that are orders of magnitude greater than the LCLS, making the European XFEL unique among hard-X-ray FELs by providing users with both high average and high peak photon fluxes.

The LCLS and XFEL are both large facilities — XFEL is approximately 3.4 km and the LCLS is around 3 km. In contrast, XFEL/SPring-8 is only 750 m; such a small facility requires extremely compact ways of generating and accelerating the electrons, as well as small FEL undulators. The electron gun in the XFEL/SPring-8 uses a single crystal of CeB_6 as a thermionic cathode, and thus differs from other X-ray FELs that use a laser to generate electrons through photoelectric emission from a 'photocathode'. Normal conducting linear accelerator cavities are driven by a 5.7 GHz radiofrequency power source. This is over four times the frequency used in FLASH/XFEL and twice that of the LCLS, which allows the cavities to be smaller and give a good accelerating gradient of around 35 MeV m^{-1}, thereby allowing a further reduction in the accelerator length for a given final beam energy. The relatively short undulator period of $\lambda_u = 18$ mm lowers the beam energy requirement for the shortest target wavelength, thus further shortening the accelerator. These short-period undulators need small magnetic pole gaps of around 3 mm to maintain a sufficient undulator magnetic field. The whole undulator must be placed inside a large vacuum chamber to allow sufficient space for the electron beam transport. These technological innovations have been demonstrated at the Spring-8 Compact SASE Source test accelerator, where FEL saturation has been achieved for wavelengths of $\lambda_1 = 51–61$ nm (ref. 55). This type of undulator is also being planned for the SwissFEL[56].

Currently, the only functioning X-ray FELs are the LCLS and the FLASH facility. Both are proposing upgrades to enrich their scientific capabilities by improving the quality of their photon output. LCLS and FLASH generate SASE FEL pulses that are both temporally and spectrally noisy. Schemes exist for 'seeding' FELs with temporally coherent pulses. Furthermore, conversion of the seed field to higher harmonics may be achieved within the FEL itself. These ideas, discussed in the next section, are proposed for implementation at LCLS-II and

FLASH-II. The ability to vary the polarization of the FEL output is also proposed, which will enable an entirely new class of experiments.

Most of the other facilities listed in Table 1 will use a range of techniques to generate FEL pulses with full temporal and transverse coherence. Polarization control will be possible at many facilities by using variably polarized undulators and possibly crossed-planar undulator schemes.

The next facility expected to come on-line is FERMI@Elettra[57] in Italy, which is currently in its commissioning phase. FERMI@Elettra comprises two FELs and will generate short pulses (25–200 fs) in the extreme ultraviolet and soft-X-ray region. The use of external laser seeding together with a harmonic up-shift scheme to obtain short wavelengths will provide temporally coherent photon pulses. This potential, in combination with the ability to temporally synchronize to external lasers and control the output photon polarization, will open up new experimental opportunities.

Future prospects

We will now consider some of the recent FEL developments and look forward to what the future may bring. There are several research fronts that are currently involved with improving and developing X-ray FEL output. Some properties, such as the peak power available at a given wavelength, seem to be more or less fixed by the FEL scaling, as determined by the ρ parameter — it is difficult to envisage a multiple order-of-magnitude change in power/efficiency similar to that provided by the high-gain FEL interaction itself.

The temporal coherence of SASE in the X-ray regime can be greatly improved. With improved temporal coherence comes improved spectral brightness, which is a measure of the number of useful photons available to the user. An obvious approach is to seed the FEL interaction using a conventional source that has good temporal coherence. If the seed power dominates the initial SASE power, the seed's coherence is maintained during the FEL amplification[58]. Although such seed sources have been successful in experiments at ~160 nm (ref. 59), current seed powers from gas-jet high-harmonic sources[60,61] limit the effective seeding to ~10 nm (ref. 58). However, methods that seed and bunch the electrons at these longer wavelengths can be used to give coherent emission at shorter, harmonic wavelengths[29,30]. Although such methods have been demonstrated[31] and are included in several proposals, insufficient seed powers at shorter wavelengths and fundamental noise amplification issues[32] suggest that these schemes are currently limited to generating coherent radiation down to the ~1 nm region[33]. However, continual improvements to high-harmonic seed lasers may allow close to Fourier-transform-limited generation — down to ~1 Å — in the coming years. Other potential methods include a 'self-seeding' scheme that spectrally filters the SASE radiation at an early stage of amplification[62], the use of 'low-charge' electron beams that generate only one near-Fourier-transform-limited SASE spike of radiation[36,63], noise suppression methods[64,65], seeded harmonic lasing[66], two-beam methods[67] and a 'temporal mixing' scheme[68]. Low-charge electron beams also have lower-emittance electron beams, which, from the emittance relation $\varepsilon_n \lesssim \gamma\lambda_1/4\pi$, means that shorter wavelength operation may be easier to achieve for a given beam energy. This is being investigated by many FEL projects. A scheme that is currently receiving much attention, and that has recently been tested in a proof-of-principle experiment, is that of echo-enabled harmonic generation[69,70]. This uses a two-stage electron energy modulation/dispersion process to achieve coherent electron bunching at high harmonics of the initial modulation frequency. The application of this technique to the X-ray regime (λ_1 = 1.5 Å) has already been modelled and seems promising[71]. Certain proposed experiments[72] predict that such schemes, if slightly modified, can even be used to generate strong seeded electron bunching at a remarkable 599th harmonic of the initial modulation laser to generate ~1.3 nm X-rays from a 160 MeV electron beam.

An alternative approach to these single-pass high-gain amplifier schemes that also generates near-transform-limited pulses is to use cavity feedback in a relatively low-gain system in an 'XFELO'[73–75]. The development of relatively high -reflectivity diamond crystal mirrors[76] in the X-ray regime makes such systems feasible. An intermediate approach identified for short-wavelength operation is to use a high-gain amplifier several gain lengths long, in a low-Q cavity[77]. Such a system also generates near-transform-limited pulses, and is referred to as a regenerative amplifier FEL. This system has been successfully demonstrated at infrared wavelengths[78] and has been investigated for short-wavelength designs[79–81]. Of significant benefit are the low requirements on cavity mirror reflectivity, with good coherence even for a low cavity feedback[82] of ~5×10^{-6}, making the design relatively robust and tolerant of cavity degradation. Unlike single-pass amplifier methods, both the XFELO and regenerative amplifier FEL design require high-repetition-rate electron pulses to match the cavity round-trip times.

Reducing X-ray pulse durations to the attosecond regime will provide spatiotemporal resolution of atomic processes[83]. Over the past decade there have been more than ten proposals for generating attosecond pulses using FELs[84–86], with none yet gaining particular preference over the others. Many of the techniques rely on the complex manipulation of the electrons in phase-space following energy modulation by external lasers, thus allowing only a short section of the electron pulse to emit radiation. Perhaps the simplest method proposed uses a short electron pulse[37] of relatively low charge in SASE mode[36], such that the number of radiation spikes emitted ($l_b/2\pi l_c$) is ~1. Simulations for the LCLS show that an electron pulse charge of only ~1 pC is required to reduce the electron pulse length sufficiently, and studies have demonstrated the generation of gigawatt peak powers in single coherent pulses of duration $\lesssim$1 fs at a wavelength of 1.5 Å (ref. 63). Experimental progress at the LCLS is being made towards this goal[87]. Two techniques have so far been reported that can take pulse durations significantly below 100 as, towards the atomic unit of time[83] of 24 as. The first uses a modified echo-enabled harmonic generation method to generate a single pulse of peak power ~200 MW and duration ~20 as at a wavelength of 1 nm[84], and the second uses a method based on mode-locking in conventional cavity lasers. Simulations show[88] that the latter technique can generate a train of pulses separated by ~150 as at a wavelength of 1.5Å, in which each pulse has a peak power of ~5 GW and a duration of ~20 as.

Further reducing FEL operating wavelengths may allow the realization of a gamma-ray FEL, which would be of significant interest for studying nuclear processes. There are, however, fundamental problems that make FEL operation at such short wavelengths more difficult. When an electron emits a photon it recoils due to the conservation of momentum. Random recoil events due to the spontaneous emission of radiation at short wavelength and high photon energy can destroy the quality of an electron beam energy spread and thus impede FEL lasing action[89]. The rate at which this 'quantum diffusion' increases as the beam propagates through the undulator scales as γ^4, and therefore limits the minimum feasible fundamental wavelength of a FEL system such as the LCLS to the $\lesssim$1 Å scale. Keeping the beam energy low and using undulators with a short period to reduce such quantum diffusion effects increases the requirements on the electron beam quality parameters (such as energy spread and emittance). New techniques are now being proposed that may enable this to be achieved[90]. Techniques that utilize harmonic methods[29,69] to allow the use of lower energy beams can also reduce the minimum wavelengths achievable. Exploiting the quantum mechanical recoil of the electrons as a positive effect has

been proposed as a way of generating narrow spectral bandwidths using a high-power laser undulator in a quantum FEL[91]. Although the short wavelength limit of a quantum FEL is still unclear, using a laser undulator would provide a significant size and cost reduction for any quantum FEL facility.

Size reductions will also be significant if recent plasma wakefield accelerator research[92] is developed to generate electron beams of sufficient beam quality for FEL lasing[93]. Now that incoherent undulator radiation has been observed[94], FEL operation is an enticing prospect. A further step in size reduction may be achieved if the source of transverse electron undulation can be incorporated within the plasma itself through the betatron oscillations induced by the focusing channel created by the plasma[95,96], which would dispense with the need for long magnetic undulators. Although incoherent X-rays have been observed[96–100], it is not yet clear if collective, coherent electron bunching — similar to that of an undulator-based FEL — is possible. One drawback of such plasma-based sources is the currently relatively low repetition rate of the drive lasers (~10 Hz) when compared with the superconducting-based linear accelerators that will drive FELs such as the European XFEL to give 2.7×10^4 pulses per second.

Even without any further development, X-ray FELs are going to have a profound impact on scientific investigations. We can expect X-ray FEL facilities to bear many new, unexpected and beautiful results over the coming years.

References

1. Kulipanov, G. N. Ginzburg's invention of undulators and their role in modern synchrotron radiation sources and free electron lasers. *Phys. Usp.* **50,** 368–376 (2007).
2. Motz, H. Applications of the radiation from fast electron beams. *J. Appl. Phys.* **22,** 527–535 (1951).
3. Motz, H., Thon, W. & Whitehurst, R. N. Experiments on radiation by fast electron beams. *J. Appl. Phys.* **24,** 826–833 (1953).
4. Phillips, R. M. History of the ubitron. *Nucl. Inst. Method. Phys. Res. A* **272,** 1–9 (1988).
5. Madey, J. M. J. Stimulated emission of bremsstrahlung in a periodic magnetic field. *J. Appl. Phys.* **42,** 1906–1913 (1971).
6. Elias, L. R., Fairbank, W. M., Madey J. M. J., Schwettman, H. A. & Smith, T. I. Observation of stimulated emission of radiation by relativistic electrons in a spatially periodic transverse magnetic field. *Phys. Rev. Lett.* **36,** 717–720 (1976).
7. Deacon, D. A. G. *et al.* First operation of a free electron laser. *Phys. Rev. Lett.* **38,** 892–894 (1977).
8. Colson, W. B. One-body electron dynamics in a free electron laser. *Phys. Lett.* **64A,** 190–192 (1977).
9. Hopf, F. A., Meystre, P., Scully, M. O. & Louisell, W. H. Classical theory of a free electron laser. *Phys. Rev. Lett.* **37,** 1215–1218 (1976).
10. Kroll, N. M. & McMullin, W. A. Stimulated emission from relativistic electrons passing through a spatially periodic transverse magnetic field. *Phys. Rev. A* **17,** 300–308 (1978).
11. Bernstein, I. B. & Hirshfield, J. L. Amplification on a relativistic electron beam in a spatially periodic transverse magnetic field. *Phys. Rev. A* **20,** 1661–1670 (1979).
12. Sprangle, P. & Smith, R. A. Theory of free electron lasers. *Phys. Rev. A* **21,** 293–301 (1980).
13. Kondratenko, A. M. & Saldin, E. L. Generation of coherent radiation by a relativistic electron beam in an ondulator. *Part. Accel.* **10,** 207–216 (1980).
14. Colson, W. B. The nonlinear wave equation for higher harmonics in free-electron lasers. *IEEE J. Quant. Electron.* **QE-17**, 1417–1427 (1981).
15. Kroll, N., Morton, P. & Rosenbluth, M. Free-electron lasers with variable parameter wigglers. *IEEE J. Quant. Electron.* **QE-17**, 1436–1468 (1981).
16. Bonifacio, R., Casagrande, F. & Casati, G. Cooperative and chaotic transition of a free electron laser Hamiltonian model. *Opt. Commun.* **40,** 219–223 (1982).
17. Bonifacio, R., Pellegrini, C. & Narducci, L. Collective instabilities and high-gain regime in a free electron laser. *Optics Commun.* **50,** 373–378 (1984).
18. Pierce, J. R. *Traveling Wave Tubes* (Van Nostrand, 1950).
19. Murphy, J. B. & Pellegrini, C. in *Laser Handbook* Vol. 6 (eds Colson, W. B. *et al.*) 9–69 (North-Holland, 1990).
20. Bonifacio, R. *et al.* Physics of the high-gain free electron laser and superradiance. *Riv. Nuovo Cimento* **13**, 1–69 (1990).
21. Saldin, E. L., Schneidmiller, E. A., Yurkov, M. V. *The physics of free electron lasers* (Springer, 2000).
22. Bratman, V. L., Ginzburg, N. S. & Petelin, M. I. Common properties of free-electron lasers. *Opt. Commun.* **30,** 409–412 (1979).
23. Bonifacio, R. & de Salvo, L. Collective atomic recoil laser (CARL): Optical gain without inversion by collective atomic recoil and self-bunching of two-level atoms. *Nucl. Inst. Meth. Phys. Res. A* **341,** 360–362 (1994).
24. Robb, G. R. M. Collective instabilities in light–matter interactions. *Proc. Les Houches Summer School* session XC (eds Dauxois, T. *et al.*) 527–544 (Oxford Univ. Press, 2010).
25. Robb, G. R. M. & McNeil, B. W. J. Superfluorescent Rayleigh scattering from suspensions of dielectric particles. *Phys. Rev. Lett.* **90,** 123903 (2003).
26. Robb, G. R. M., McNeil, B. W. J., Galbraith, I. & Jaroszynski, D. A. Collective free-carrier scattering in semiconductors. *Phys. Rev. B* **63,** 165208 (2001).
27. Acebrón, J. A. *et al.* The Kuramoto model: A simple paradigm for synchronization phenomena. *Rev. Mod. Phys.* **77,** 137–185 (2005).
28. Clarke, J. A. *The science and technology of undulators and wigglers* (Oxford University Press, 2004).
29. Bonifacio, R., de Salvo Souza, L., Pierini, P. & Scharlemann, E. T. Generation of XUV light by resonant-frequency tripling in a 2-wiggler FEL amplifier. *Nucl. Inst. Meth. Phys. Res. A* **296,** 787–790 (1990).
30. Yu L. H. Generation of intense UV radiation by subharmonically seeded single-pass free-electron lasers. *Phys. Rev. A* **44,** 5178–5193 (1991).
31. Doyuran, A. *et al.* Characterization of a high-gain harmonic-generation free-electron laser at saturation. *Phys. Rev. Lett. 86,* 5902–5905 (2001).
32. Saldin, E. L., Schneidmiller, E. A. & Yurkov, M. V. Study of a noise degradation of amplification process in a multistage HGHG FEL. *Opt. Commun.* **202,** 169–187 (2002).
33. Dunning, D. J. *et al.* Optimisation of an HHG-seeded harmonic cascade FEL design for the NLS project. *Proc. 1st Int. Particle Accelerator Conf.* **TUPE049,** 2254–2256 (2010).
34. Kim, K.-J. Three-dimensional analysis of coherent amplification and self-amplified spontaneous emission in free-electron lasers. *Phys. Rev. Lett.* **57,** 1871–1874 (1986).
35. Siegman, A. E. *Lasers* (University Science Books, 1986).
36. Bonifacio, R., de Salvo, L., Pierini, P., Piovella, N. & Pellegrini, C. Spectrum, temporal structure, and fluctuations in a high-gain free-electron laser starting from noise. *Phys. Rev. Lett.* **73,** 70–73 (1994).
37. Bonifacio, R., McNeil, B. W. J. & Pierini, P. Superradiance in the high-gain free-electron laser. *Phys. Rev. A* **40,** 4467–4475 (1989).
38. http://fel09.dl.ac.uk/documents/Lectures/tutorial/Emma-SUPA-Tutorial-Lecture.ppt.
39. Humphries, S. Jr *Charged Particle Beams* Ch. 3, 79–132 (Wiley, 1990).
40. Kim, K.-J. Brightness, coherence and propagation characteristics of synchrotron radiation. *Nucl. Inst. Meth. Phys. Res. A* **246** 71–76 (1986).
41. Scharlemann, E. T. Wiggle plane focusing in linear wigglers. *J. Appl. Phys.* **58,** 2154–2161 (1985).
42. Faatz, B. & Pflüger, J. Different focusing solutions for the TTF-FEL undulator. *Nucl. Inst. Meth. Phys. Res. A* **475** 603–607 (2001).
43. Scharlemann, E. T. in *High gain, high power FEL* (eds Bonifacio, R. *et al.*) 95 (Elsevier, 1989).
44. Bonifacio, R., de Salvo Souza, L. & McNeil, B. W. J. Emittance limitations in the free electron laser. *Opt. Commun.* **93,** 179–185 (1992).
45. Scharlemann, E. T., Sessler, A. M. & Wurtele, J. S. Optical guiding in a free-electron laser. *Phys. Rev. Lett.* **54,** 1925–1928 (1985).
46. Li, Y., Faatz, B. & Pflueger, J. Undulator system tolerance analysis for the European X-ray free-electron laser. *Phys. Rev. Spec. Top. AB* **11,** 100701 (2008).
47. Nuhn, H.-D. LCLS undulator commissioning, alignment and performance. *Proc. 31st Int. Free Electron Laser Conf.* **THOA02,** 714–721 (2009).
48. Huang, Z., Kim, K.-J. Review of X-ray free-electron laser theory. *Phys. Rev. Spec. Top. AB* **10,** 034801 (2007).
49. Robinson, I. *et al.* Focus on X-ray beams with high coherence. *New J. Phys.* **12,** 035002 (2010).
50. Colson W. B. *et al.* Free electron lasers in 2009. *Proc. 31st Int. Free Electron Laser Conf.* **WEPC43,** 591–595 (2009).
51. Emma, P. *et al.* First lasing and operation of an ångstrom-wavelength free-electron laser. *Nature Photon.* **4,** 641–647 (2010).
52. Altarelli, M. *et al.* (eds). XFEL: The European X-ray free-electron laser technical design report. DESY 2006-097 (DESY, 2007).
53. Shintake, T. *et al.* Status report on Japanese XFEL construction project at SPring-8. *Proc. 1st Int. Particle Accelerator Conf.* **TUXRA02,** 1285–1289 (2010).
54. Faatz, B. *et al.* FLASH II: A seeded future at FLASH. *Proc. 1st Int. Particle Accelerator Conf.* **TUPE005,** 2152–2154 (2010).
55. Shintake, T. *et al.* A compact free-electron laser for generating coherent radiation in the extreme ultraviolet region. *Nature Photon.* **2,** 555–559 (2008).

56. Patterson, B. D. *et al.* Coherent science at the Swiss FEL X-ray laser. *New J. Phys.* **12**, 035012 (2010).
57. Penco, G. The FERMI@ETETTRA commissioning. *Proc. 1st Int. Particle Accelerator Conf.* **TUOARA02,** 1293–1295 (2010).
58. McNeil, B. W. J. *et al.* An XUV-FEL amplifier seeded using high harmonic generation. *New J. Phys.* **9,** 82 (2007).
59. G. Lambert. *et al.* Injection of harmonics generated in gas in a free-electron laser providing intense and coherent extreme-ultraviolet light. *Nature Phys.* **4,** 296–300 (2008).
60. Ferray, M. *et al.* Multiple-harmonic conversion of 1064 nm radiation in rare gases. *J. Phys. B* **21**, L31–L35 (1988).
61. McPherson, A. *et al.* Studies of multiphoton production of vacuum-ultraviolet radiation in the rare gases. *J. Opt. Soc. Am. B* **4,** 595–601 (1987).
62. Ding, Y., Huang, Z. & Ruth, R. D. Two-bunch self-seeding for narrow-bandwidth hard X-ray free-electron lasers. *Phys. Rev. Spec. Top. AB* **13,** 060703 (2010).
63. Reiche, S., Musumeci, P., Pellegrini, C. & Rosenzweig, J. B. Development of ultra-short pulse, single coherent spike for SASE X-ray FELs. *Nucl. Inst. Meth. Phys. Res. A* **593,** 45–48 (2008).
64. Gover, A. & Dyunin, E. Collective-interaction control and reduction of optical frequency shot noise in charged-particle beams. *Phys. Rev. Lett.* **102,** 154801 (2009).
65. Litvinenko, V. N. Suppressing shot noise and spontaneous radiation in electron beams. *Proc. 31st Int. Free Electron Laser Conf.* **TUOB05,** 229–234 (2009).
66. McNeil, B. W. J., Robb, G. R. M., Poole, M. W. & Thompson, N. R. Harmonic lasing in a free-electron-laser amplifier. *Phys. Rev. Lett.* **96,** 084801 (2006).
67. McNeil, B. W. J., Robb, G. R. M. & Poole, M. W. Two-beam free-electron laser. *Phys. Rev. E* **70,** 035501(R) (2004).
68. Thompson, N. R., Dunning, D. J. & McNeil, B. W. J. Improved temporal coherence in SASE FELs. *Proc. 1st Int. Particle Accelerator Conf.* **TUPE050,** 2257–2259 (2010).
69. Stupakov, G. Using the beam-echo effect for generation of short-wavelength radiation. *Phys. Rev. Lett.* **102,** 074801 (2009).
70. Xiang, D. *et al.* Demonstration of the echo-enabled harmonic generation technique for short-wavelength seeded free electron lasers. *Phys. Rev. Lett.* **115,** 114801 (2010).
71. Xiang, D., Huang, Z., Ratner, D. & Stupakov, G. Feasibility study for a seeded hard X-ray source based on a two-stage echo-enabled harmonic generation FEL. *Proc. 31st Int. Free Electron Laser Conf.* **MOPC79,** 192–195 (2009).
72. Feng, C. & Zhao, Z. T. Coherent hard X-ray free-electron laser based on echo enabled staged harmonic generation scheme. *Proc. 1st Int. Particle Accelerator Conf.* **TUPD092,** 2120–2122 (2010).
73. Colella, R. & Luccio, A. Proposal for a free electron laser in the X-ray region. *Opt. Commun.* **50,** 41–44 (1984).
74. Kim, K.-J., Shvyd'ko, Y. & Reiche, S. An X-ray free-electron laser oscillator with an energy recovery linac. *Phys. Rev. Lett.* **100,** 244802 (2008).
75. Kim, K.-J. & Shvyd'ko, Y. Tunable optical cavity for an X-ray free-electron-laser oscillator. *Phys. Rev. Spec. Top. AB* **12,** 030703 (2009).
76. Shvyd'ko, Y. V. *et al.* High-reflectivity high-resolution X-ray crystal optics with diamonds. *Nature Phys.* **6,** 196–199 (2010).
77. McNeil, B. W. J. A simple model of the free-electron-laser oscillator from low into high gain. *IEEE J. Quant. Electron.* **26,** 1124–1129 (1990).
78. Nguyen, D. C. *et al.* First lasing of the regenerative amplifier FEL. *Nucl. Inst. Meth. Phys. Res. A* **429,** 125–130 (1999).
79. Faatz, B. *et al.* Regenerative FEL amplifier at the TESLA test facility at DESY. *Nucl. Inst. Meth. Phys. Res. A* **429,** 424–428 (1999).
80. Huang, Z. & Ruth, R. Fully coherent X-ray pulses from a regenerative-amplifier free-electron laser. *Phys. Rev. Lett.* **96,** 144801 (2006).
81. McNeil, B. W. J. *et al.* A design for the generation of temporally-coherent radiation pulses in the VUV and beyond by a self-seeding high-gain free electron laser amplifier. *New J. Phys.* **9,** 239 (2007).
82. Dunning, D. J., McNeil, B. W. J. & Thompson, N. R. Short wavelength regenerative amplifier free electron lasers. *Nucl. Inst. Meth. Phys. Res. A* **593,** 116–119 (2008).
83. Krausz, F. & Ivanov, M. Attosecond physics. *Rev. Mod. Phys.* **81,** 163–234 (2009).
84. Xiang, D., Huang, Z. & Stupakov, G. Generation of intense attosecond X-ray pulses using ultraviolet laser induced microbunching in electron beams. *Phys. Rev. Spec. Top. AB* **12,** 060701 (2009).
85. Ding. Y. *et al.* Generation of attosecond X-ray pulses with a multicycle two-color enhanced self-amplified spontaneous emission scheme. *Phys. Rev. Spec. Top. AB* **12,** 060703 (2009).
86. Penn, G. & Zholents, A. Synchronized attosecond pulses for X-ray spectroscopy. *Proc. 31st Int. Free Electron Laser Conf.* **MOPC73,** 176–179 (2009).
87. Ding, Y. *et al.* Measurements and simulations of ultralow emittance and ultrashort electron beams in the Linac Coherent Light Source. *Phys. Rev. Lett.* **102,** 254801 (2009).
88. Thompson, N. R. & McNeil, B. W. J. Mode locking in a free-electron laser amplifier. *Phys. Rev. Lett.* **100,** 203901 (2008).
89. Rossbach, J., Saldin, E. L., Schneidmiller, E. A. & Yurkov. M. V. Fundamental limitations of an X-ray FEL operation due to quantum fluctuations of undulator radiation. *Nucl. Inst. Meth. Phys. Res. A* **393,** 152–l 56 (1997).
90. Xiang, D. Laser assisted emittance exchange: Downsizing the X-ray free electron laser. *Phys. Rev. Spec. Top. AB* **13,** 010701 (2010).
91. Bonifacio, R., Piovella, N., Robb, G. R. M. & Schiavi, A. Quantum regime of free electron lasers starting from noise. *Phys. Rev. Spec. Top. AB* **9,** 090701 (2006).
92. Malka, V. *et al.* Principles and applications of compact laser–plasma accelerators. *Nature Phys.* **4,** 447–453 (2008).
93. Grüner, F. *et al.* Design considerations for table-top, laser-based VUV and X-ray free electron lasers. *Appl. Phys. B* **86,** 431–435 (2007).
94. Schlenvoigt, H.-P. *et al.* A compact synchrotron radiation source driven by a laser-plasma wakefield accelerator. *Nature Phys.* **4,** 130–133 (2007).
95. Esarey, E., Shadwick, B. A., Catravas, P. & Leemans W. P. Synchrotron radiation from electron beams in plasma-focusing channels. *Phys. Rev. E* **65,** 056505 (2002).
96. Thomas, A. G. R. & Krushelnick, K. Betatron X-ray generation from electrons accelerated in a plasma cavity in the presence of laser fields. *Phys. Plasmas* **16,** 103103 (2009).
97. Rousse, A. *et al.* Production of a keV X-ray beam from synchrotron radiation in relativistic laser–plasma interaction. *Phys. Rev. Lett.* **93,** 135005 (2004).
98. Phuoc, K. T. *et al.* Imaging electron trajectories in a laser-wakefield cavity using betatron X-ray radiation. *Phys. Rev. Lett.* **97,** 225002 (2006).
99. Dorchies, F. *et al.* Observation of subpicosecond X-ray emission from laser–cluster interaction. *Phys. Rev. Lett.* **100,** 205002 (2008).
100. Kneip, S. *et al.* Observation of synchrotron radiation from electrons accelerated in a petawatt-laser-generated plasma cavity. *Phys. Rev. Lett.* **100,** 105006 (2008).
101. Schreiber, S. *et al.* FEL user facility FLASH. *Proc. 1st Int. Particle Accelerator Conf.* **TUPE004,** 2149–2151 (2010).
102. Kim E.-S. & Yoon M. Beam dynamics in a 10-GeV linear accelerator for the X-Ray free electron laser at PAL. *IEEE T. Nucl. Sci.* **56,** 3597–3606 (2009).
103. https://slacportal.slac.stanford.edu/sites/lcls_public/lcls_ii/Pages/default.aspx.
104. Palumbo, L. The SPARX FEL project. *Proc. 1st Int. Particle Accelerator Conf.* **TUPE022,** 2185–2187 (2010).

Additional information

The authors declare no competing financial interests.